Supplementary information

"Lignin-First" biorefinery towards efficient aromatic monomer conversion from coconut shells using mild TMAH-based alkaline deep eutectic solvents

Chenjun He[a], Fengqi Luo[a], Yongzhi Zhu[a], Ao Zhan[a], Jiajun Fan[c], James H. Clark[c], Jie Lv[b,*] Qiang Yu[a,*]

[a]*South China Agricultural University, Institute of Biomass Engineering, Key Laboratory of Energy Plants Resource and Utilization, Ministry of Agriculture and Rural Affairs, Guangdong Engineering Technology Research Center of Agricultural and Forestry Biomass, Guangzhou 510642, China*

[b]*Guangdong Polytechnic Normal University, School of Mechatronic Engineering, Guangzhou 510450, China*

[c]*Green Chemistry Centre of Excellence, Department of Chemistry, University of York, York, YO10 5DD, UK*

[*]Co-*Corresponding author*

Qiang Yu, E-mail address: yuqiang@scau.edu.cn

Content list:

Supplementary materials and methods:

The milled wood lignin (MWL) was extracted by ball milling and 1,4-dioxane/water (96/4, v/v) solvent system. In detail, the cocoanut shells after 24 h ball milling were reacted with 1,4-dioxane/water (96/4, v/v) at 80℃ for 12 h to extract lignin. After the reaction, the mixture was solid-liquid separated via Vacuum filtration to obtain the liquid fraction rich in lignin. Then, the liquid part was rotary evaporation at 60℃ for removing water and 1,4-dioxane. To further purify the lignin, dissolve it with acetic acid/water (9:1, v/v) and add the slurry to water to precipitate the lignin. Subsequently, the precipitated lignin was washed to neutral and vacuum-dried for future structural characterization.

The cellulose and hemicellulose recovery, delignification ratio are calculated based on the chemical compositions of the untreated sample according to the following eqs:[1]

$$\text{Cellulose recovery (\%)} = \frac{\textit{The weight of}\ \text{cellulose in treated sample}\ (g)}{\textit{The weight of}\ \text{cellulose in}\ \textit{un}\text{treated sample}\ (g)} \times 100\% \quad \text{(S1)}$$

$$\text{Hemicellulose recovery (\%)} = \frac{\textit{The weight of hemi}\text{cellulose in treated sample}\ (g)}{\textit{The weight of hemi}\text{cellulose in treated sample}\ (g)} \times 100\% \quad \text{(S2)}$$

$$\text{Delignification ratio (\%)} = 1 - \frac{\textit{The weight of}\ \text{lignin in treated sample}\ (g)}{\textit{The weight of}\ \text{lignin in}\ \textit{un}\text{treated sample}\ (g)} \times 100\% \quad \text{(S3)}$$

The ^{1}H nuclear magnetic resonance (NMR) of solvent was determined by an NMR spectrometer (AV II 600 MHz spectrometer, Bruker, Germany). The HBA, HBD and the prepared solvent were dissolved in DMSO-d6 for determining. Since lysine is insoluble in DMSO, D_2O was employed for dissolving it.

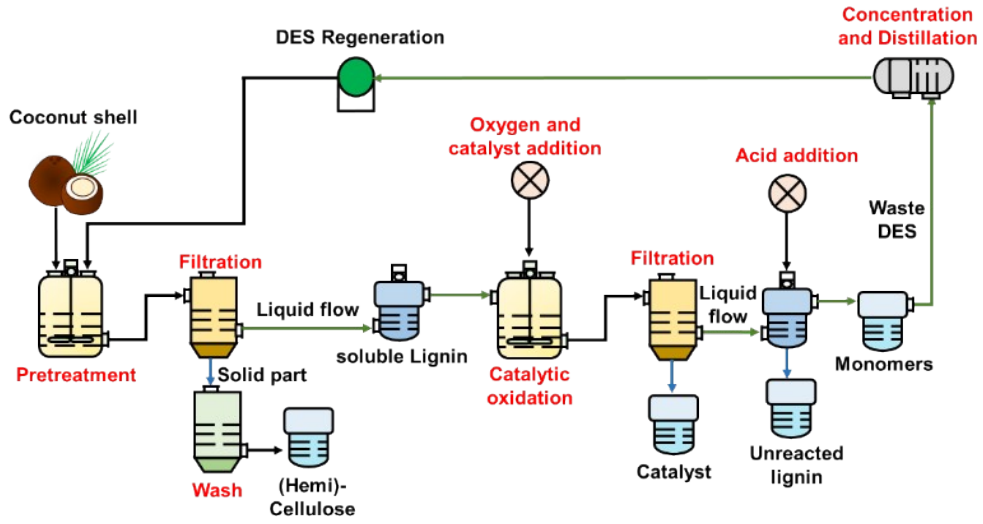

Fig. S1 Technical route of lignocellulose fraction and depolymerization.

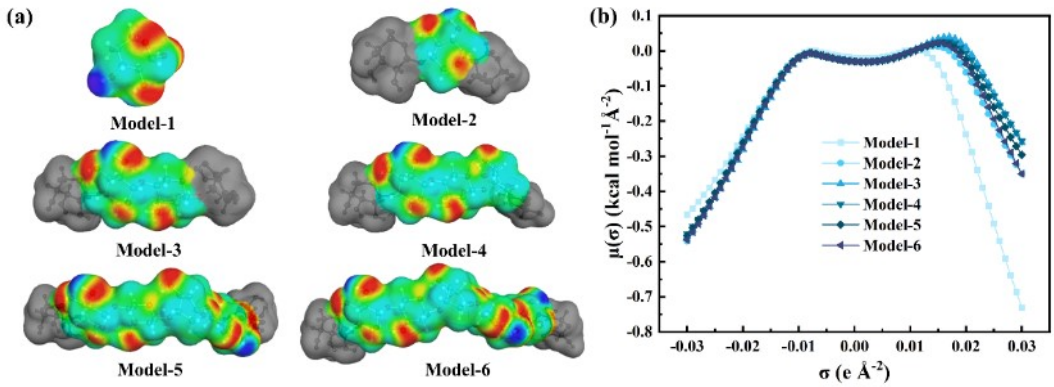

Fig. S2 COSMO-RS charge surfaces (a) and (b) σ-potentials of hemicellulose models (Model-1: xylose; Model-2: mid-monomer of xylotriose; Model-3: mid-dimer of xylotetrose; Model-4: mid-trimer of xylopentose; Model-5: mid-tetramer of xylohexose; Model-6:mid-pentamer of xyloheptose) predicted by COSMO-RS. In a, the extent of the screening charge varies from –0.03 e $Å^{-2}$ to +0.03 e $Å^{-2}$. Red and blue represent positive and negative surface screening charges, respectively, and green represents neutral charges.

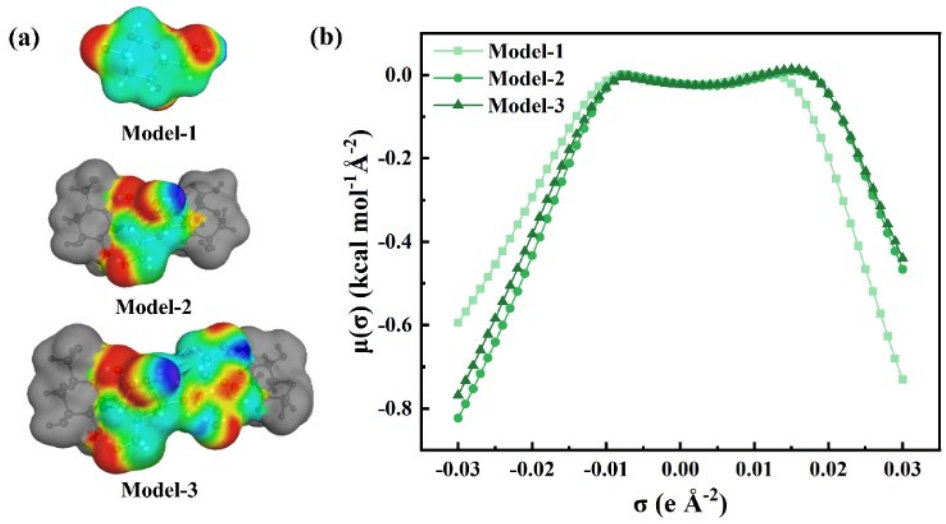

Fig. S3 COSMO-RS charge surfaces (a) and (b) σ-Potentials of cellulose models (Model-1: glucose; Model-2: mid-monomer of glucotriose; Model-3: mid-dimer of glucotetrose) predicted by COSMO-RS. In a, the extent of the screening charge varies from –0.03 e $Å^{-2}$ to +0.03 e $Å^{-2}$. Red and blue represent positive and negative surface screening charges, respectively, and green represents neutral charges.

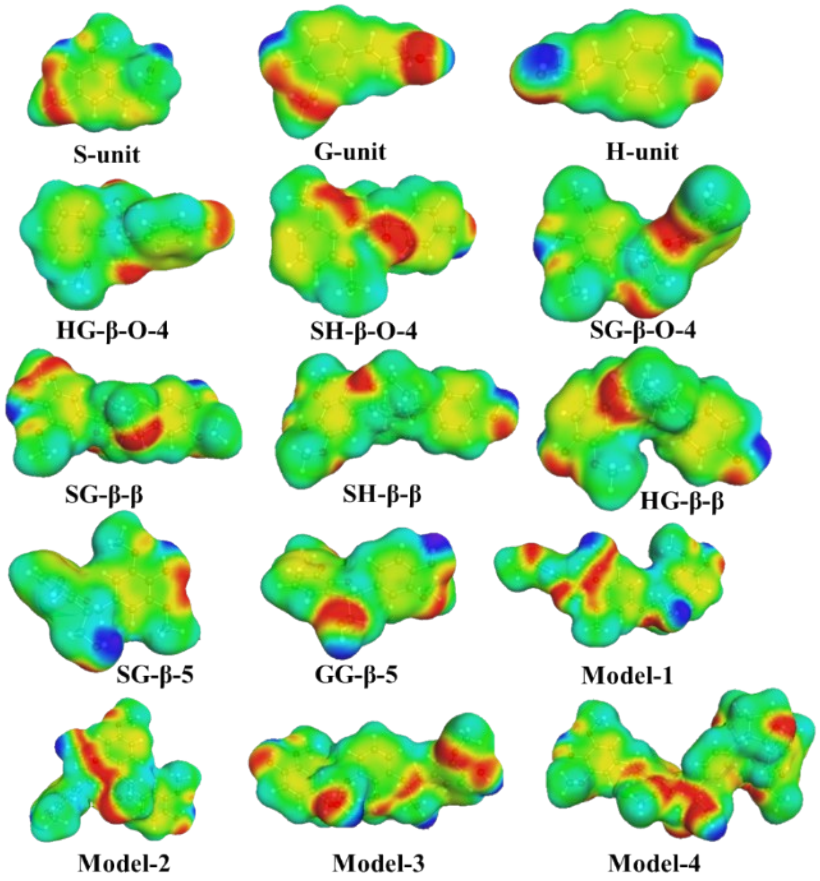

Fig. S4 COSMO-RS charge surfaces of lignin models (S-unit; G-unit; H-unit; HG-β-O-4: H-unit and G-unit connected by β-O-4 linkage; SH-β-O-4: S-unit and H-unit connected by β-O-4 linkage; SG-β-O-4: S-unit and G-unit connected by β-O-4 linkage; SG-β-β: S-unit and G-unit connected by β-β linkage; SH-β-β: S-unit and H-unit connected by β-β linkage; HG-β-β: H-unit and G-unit connected by β-β linkage; SG-β-5: S-unit and G-unit connected by β-5 linkage; GG-β-5: G-unit and G-unit connected by β-5 linkage; Model-1, Model-2 and Model-3: three unit connected by β-O-4 at different benzene ring locations; Model-4: four unit connected by three types of linkages) built by COSMO-RS. The extent of the screening charge varies from –0.03 e $Å^{-2}$ to +0.03 e $Å^{-2}$. Red and blue represent positive and negative surface screening charges, respectively, and green represents neutral charges.

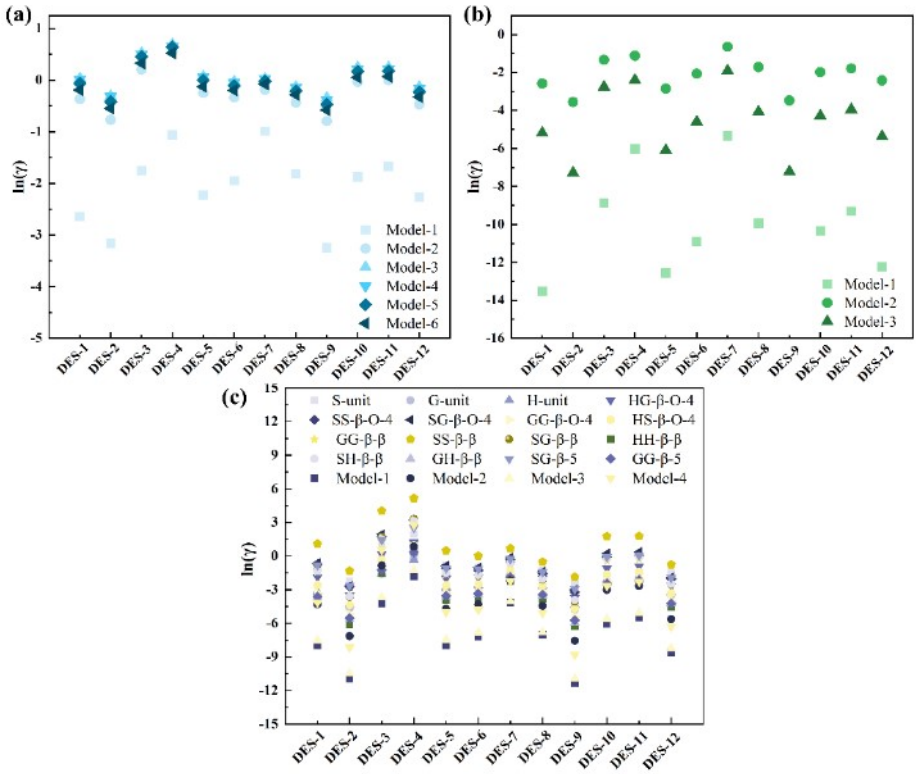

Fig. S5 Activity coefficients of lignocellulosic models in different solvent systems (Take 12 of these solvents as examples) (120°C): (a) hemicellulose, (b) cellulose, and (c) lignin.

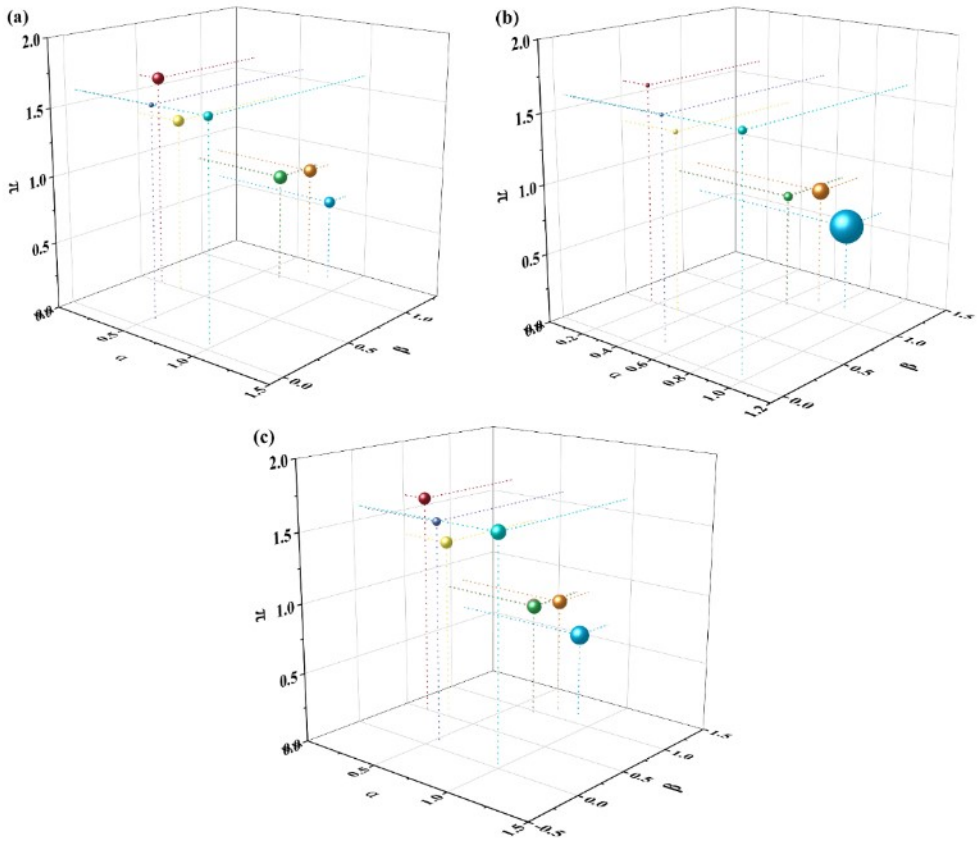

Fig. S6 The correlation between lignin solubility and the Kamlet−Taft parameters of solvents: (a) hemicellulose, (b) cellulose and (c) lignin. The size of the ball indicates the solubility.

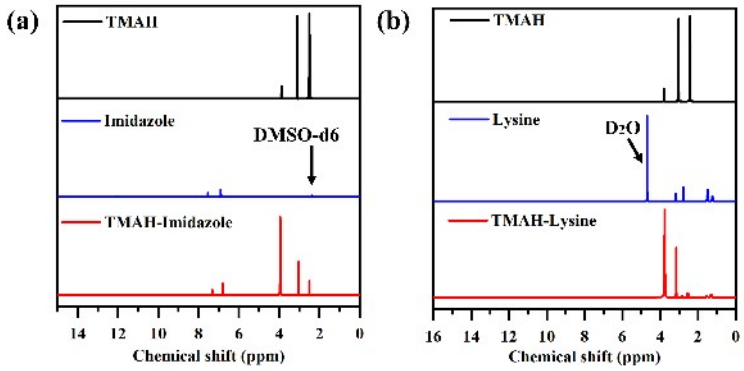

Fig. S7 ^{1}H NMR of TMAH-based DESs: (a) TMAH-Imidazole and (b) TMAH-Lysine.

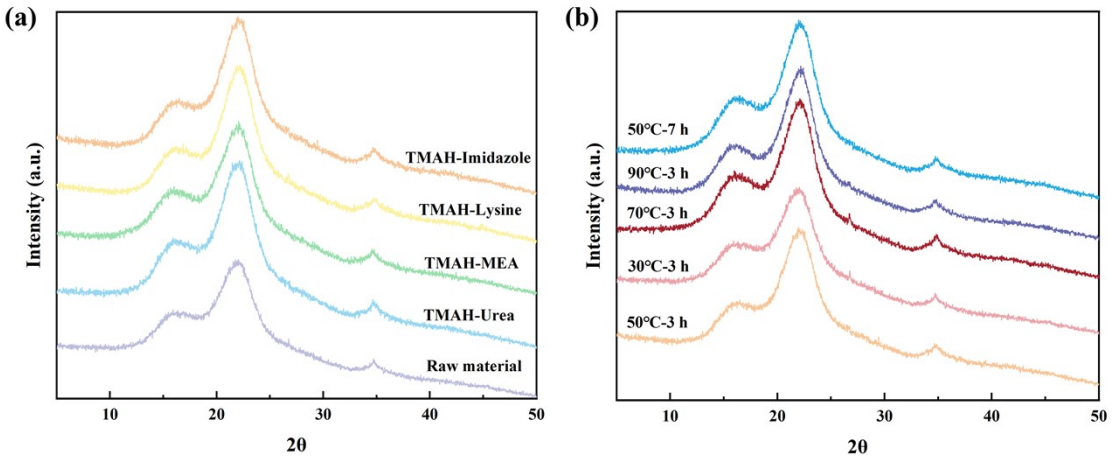

Fig. S8 XRD pattern of (a) raw material and the substrates treated by different DESs (50℃, 3 h) and (b) the substrates treated by TMAH-Imidazole at different conditions.

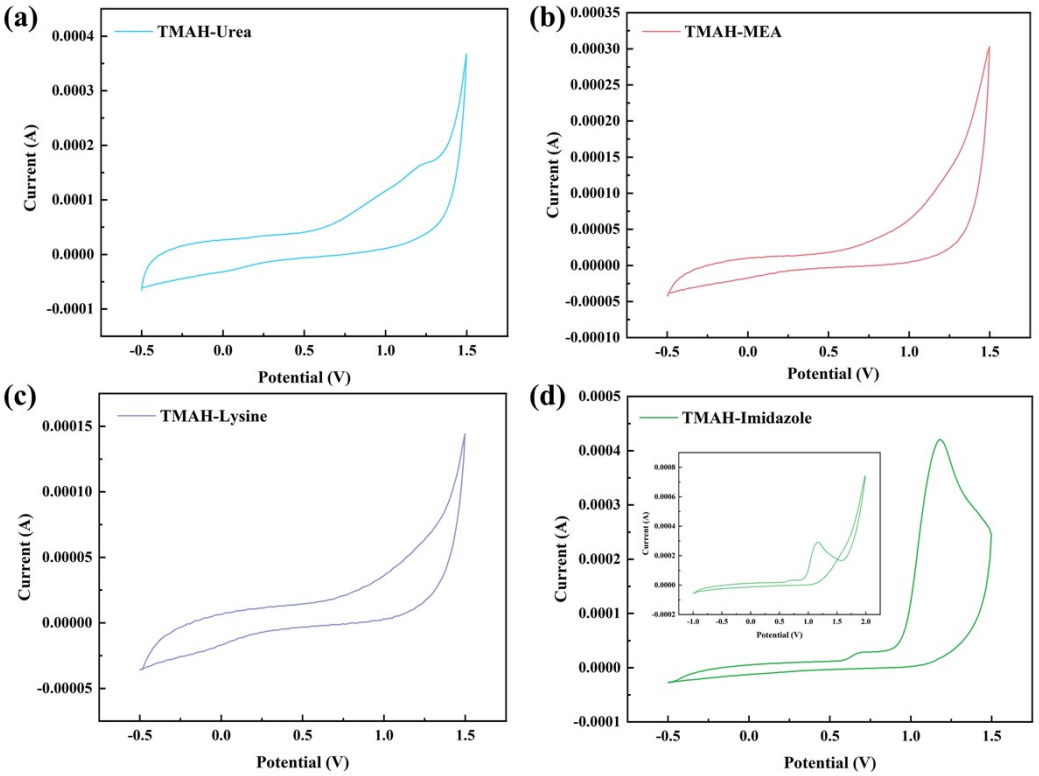

Fig. S9 Cyclic voltammetry curves of TMAH-based DESs at scan rate of 20 mV s^{-1}.

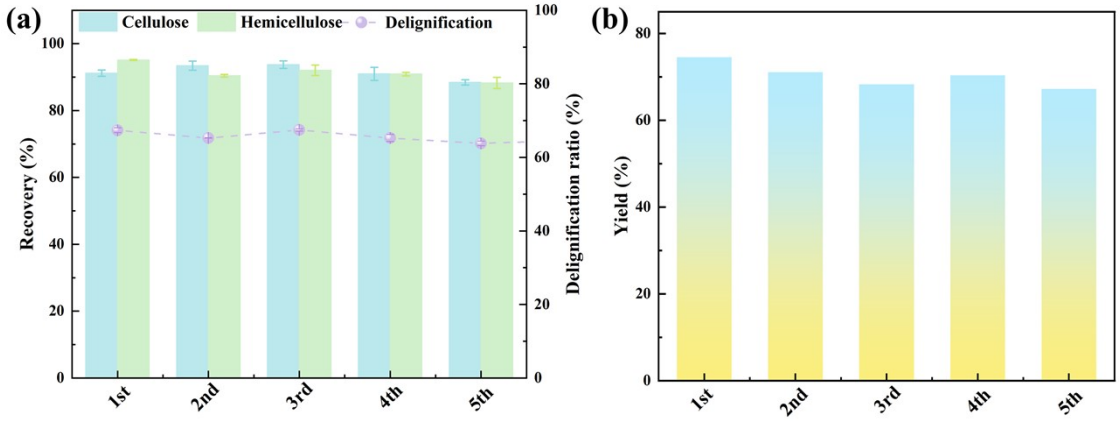

Fig. S10 Reusability of DES: (a) delignification ratio and Carbohydrate recovery; (b) aromatic monomers yield.

Table S1 The information of hydrogen bond donors and hydrogen bond acceptors for preparing DESs.

Hydrogen bond acceptor	Hydrogen bond donor	Molar ratio
ChCl/[TMAH]Cl/[TEA]Cl/ [TMAH]Br/[TEA]Br/ChOH/ Betaine/TMAH/TEAH	Arginine	1:1
	Lysine	1:1
	Histdine	1:1
	Thiourea	1:2
	Urea	1:2
	MEA	1:6
	DEA	1:6
	IPPA	1:6
	EDM	1:6
	Imidazole	3:7
	Pyrazole	3:7
	Pyridine	3:7
	Pyrrole	3:7
[TPA]Cl/[BTMA]Cl/ [TPA]Br/[BTMA]Br/ TPAH/ BTAH	Arginine	1:2
	Lysine	1:2
	Histdine	1:2
	Thiourea	1:4
	Urea	1:4
	MEA	1:12
	DEA	1:12
	IPPA	1:12
	EDM	1:12
	Imidazole	3:14
	Pyrazole	3:14
	Pyridine	3:14
	Pyrrole	3:14

ChCl: Choline chloride (ChCl), [TMAH]Cl: Tetramethylene ammonium chloride, [TEA]Cl: Tetraethylammonium chloride, [TPA]Cl: Tetrapropyl ammonium chloride, [BTMA]Cl: Tetrabutylammonium chloride, [TMAH]Br: Tetramethylammonium bromide, [TEA] Br: Tetraethylammonium bromide, [TPA]Br: Tetrapropyl ammonium bromide, [BTMA]Br: Tetrabutylammonium bromide, ChOH: Choline hydroxide, TMAH: Tetramethylammonium hydroxide, TEAH: Tetraethylammonium hydroxide, TPAH: Tetrapropyl ammonium hydroxide, BTAH: Tetrabutylammonium hydroxide; MEA: Monoethanolamine, DEA: Diethanolamine, IPPA: Isopropanolamine, EDM: Ethylenediamine.

Table S2 Comparison of the lignocellulose fractionation effect of TMAH-based solvents for reported alkaline DESs

Solvent type	Material	Reaction condition	Cellulose recovery	Hemicellulose recovery	Delignification	Ref.
K_2CO_3-Glycerol (1:7)	Bamboo	130℃, 3 h	95%	65%	55%	[2]
K_2CO_3-Glycol (1:7)	Coconut shell	130℃, 1 h	86.5%	70.2%	70.7%	[1]
Ethanolamine-ChCl (6:1)	Bamboo	70℃, 9 h	90.7%	80%	45%	[3]
Imidazole-ChCl (7:3)	Populus	150℃, 15 h	69.2%	18.3%	75.5%	[4]
Urea-ChCl (2:1)	Populus	115℃, 15 h	84.5%	79.1%	20.0%	[4]
50% Urea-ChOH (2:1)	Rice straw	100℃, 2 h	85%	5%	>90%	[5]
30% Imidazole-TMAH (7:3)	Coconut shell	50℃, 3 h	91.2%	95.1%	67.4%	This work
30% Imidazole-TMAH (7:3)	Coconut shell	90℃, 3 h	86.9%	80.3%	75.5%	This work

Table S3 The NMR assignments of major signals in the 2D-HSQC spectra of MWL and DES extracted lignin.

Label	δ_C/δ_H (ppm)	Assignment
C_β	53.0/3.45	C_β–H_β in phenylcoumarane substructures (C)
B_β	53.5/3.03	C_β–H_β in *β*-*β* (resinol) substructures (B)
-OCH_3	55.2/3.74	C–H in methoxyls
A_γ	59.7/3.21–3.71	C_γ–H_γ in *β*-*O*-4 substructures (A)
A'_γ	63.0/4.30	C_γ–H_γ in γ-acylated *β*-*O*-4 substructures (A)
I_γ	61.7/4.09	C_γ–H_γ in cinnamyl alcohol end-groups (I)
C_γ	62.7/3.67	C_γ–H_γ in phenylcoumaran substructures (C)
B_γ	71.2/3.85–4.16	C_γ–H_γ in *β*-*β* (resinol) substructures (B)
A_α	71.8/4.86	C_α–H_α in *β*-*O*-4 linked to S units (A)
$A_{\beta(G)}$/ $A'_{\beta(S)}$	83.5/4.27	C_β–H_β in *β*-*O*-4 substructures linked to G and H units (A)
B_α	85.1/4.62	C_α–H_α in *β*-*β* (resinol) substructures (B)
$A'_{\beta(G)}$	83.1/4.48	C_β–H_β in acylated *β*-*O*-4 substructures linked to G units (A)
$A_{\beta(S)}$	86.0/4.11	C_β–H_β in *β*-*O*-4 substructures linked to S units (A)
C_α	86.8/5.42	C_α–H_α in phenylcoumaran substructures (C)
$S_{2,6}$	103.4/6.68	$C_{2,6}$–$H_{2,6}$ in etherified syringyl units (S)
FA_2	110.6/7.32	C_2–H_2 in ferulate (FA)
G_2	110.5/6.92	C_2–H_2 in guaiacyl units (G)
PCE_8	114.6/6.29	C_8–H_8 in *p*-coumarate (PCE)
G_5	114.7/6.71	C_2–H_2 in guaiacyl units (G)
G_6	118.8/6.75	C_6–H_6 in guaiacyl units (G)
$H_{2,6}$	127.8/7.16	$C_{2,6}$–$H_{2,6}$ in *p*-hydroxyphenyl units (H)
$PCE_{2,6}$	130.2/7.49	$C_{2,6}$–$H_{2,6}$ in *p*-coumarate (PCE)
$PB_{2,6}$	131.3/7.66	$C_{2,6}$–$H_{2,6}$ in *p*-hydroxybenzoate substructures (PB)

Table S4 Comparison of the yield of aromatic monomers of TMAH-Imidazole for reported solvents.

Substrate	Catalyst/Solvent	Reaction condition	Yield	Reference
Industrial lignin	MnO_2/Methanol	140℃, 1 h, 1 Mpa O_2	38% (bio-oil)	[6]
Industrial lignin	CeO_2/Methanol	140℃, 1 h, 1 Mpa O_2	48% (bio-oil)	[6]
Industrial lignin	MoO/Methanol	140℃, 1 h, 1 Mpa O_2	40% (bio-oil)	[6]
Alkali lignin	CuO/NaOH	160℃, 1 h 1atm O_2	13.9%	[7]
Pine	CuO/NaOH	160℃, 1 h, 1 Mpa O_2	33.8.6%	[7]
Pine	Fe_3O_4 /NaOH	160℃, 1 h, 1 Mpa O_2	25%	[7]
Pine	Al_2O_3 /NaOH	160℃, 1 h, 1 Mpa O_2	23%	[7]
Lignin	CuO-$Fe_2(SO_4)_3$/NaOH-MeOH	150℃, 1 h, 2 mL H_2O_2 (30 wt.%)	17.92%	[8]
Dealkali lignin	SiO_2−Al_2O_3 H_2O/MeOH	250°C, 30 min, 0.7 MPa of N_2,	58%	[9]
Bamboo	$CuSO_4$-Fe_2O_3/NaOH	195 °C, 1.5 h, 0.6 Mpa O_2	40.3% (bio-oil)	[10]
Kraft Lignin	Mn-sepiolite/Supercritical ethanol	290°C, 4 h, 0.6 Mpa O_2	~40%	[11]
DES-extracted lignin	MnO_2/TMAH-Imidazole	100°C, 2 h, 1 Mpa O_2	74.54%	This work

Reference

1 C. He, X. Li, F. Luo, C. Mi, A. Zhan, R. Ou, J. Fan, J. H. Clark and Q. Yu, *ACS Sustain. Chem. Eng.*, 2024, **12**, 11327–11337.

2 F. Shen, S. Wu, M. Huang, L. Zhao, J. He, Y. Zhang, S. Deng, J. Hu, D. Tian and F. Shen, *Green Chem.*, 2022, 5242–5254.

3 Y. Guo, L. Xu, F. Shen, J. Hu, M. Huang, J. He, Y. Zhang, S. Deng, Q. Li and D. Tian, *Chemosphere*, 2022, **286**, 131798.

4 H. Li, X. Li, T. You, D. Li, H. Nawaz, X. Zhang and F. Xu, *Int. J. Biol. Macromol.*, 2021, **193**, 319–327.

5 Y. Jiang, F. Shen, B. Jiang, Y. Hu, J. Hu, M. Huang, L. Zhao, H. Wu, D. Tian and F. Shen, *Chem. Eng. J.*, 2024, **479**, 147610.

6 A. Kumar, B. Biswas, R. Kaur, S. Rawat, B. B. Krishna, P. Kumbhar, S. Pal, S. Padmanabhan and T. Bhaskar, *Bioresour. Technol.*, 2022, **352**, 127032.

7 Y. Zhu, Y. Liao, L. Lu, W. Lv, J. Liu, X. Song, J. Wu, L. Li, C. Wang, L. Ma and B. F. Sels, *ACS Catal.*, 2023, **13**, 7929–7941.

8 X. Ouyang, T. Ruan and X. Qiu, *Fuel Process. Technol.*, 2016, **144**, 181–185.

9 A. K. Deepa and P. L. Dhepe, *ACS Catal.*, 2015, **5**, 365–379.

10 C. S. McCallum, W. Wang, W. J. Doran, W. G. Forsythe, M. D. Garrett, C. Hardacre, J. J. Leahy, K. Morgan, D. S. Shin and G. N. Sheldrake, *Green Chem.*, 2021, **23**, 1847–1860.

11 M. Chen, W. Dai, Y. Wang, Z. Tang, H. Li, C. Li, Z. Yang and J. Wang, *Fuel*, 2023, **333**, 126365.